Robust 1D inversion of large towed geo-electric array datasets used for hydrogeological studies*

David Allen[1,3] Noel Merrick[2]

[1]Groundwater Imaging Pty. Ltd., 279 Fitzroy St, Dubbo NSW 2830, Australia.

[2]National Centre for Groundwater Management, University of Technology Sydney, Sydney NSW 2007, Australia.

[3]Corresponding author. Email: David@GroundwaterImaging.com

Abstract. The advent of towed geo-electrical array surveying on water and land has resulted in datasets of magnitude approaching that of airborne electromagnetic surveying and most suited to 1D inversion. Robustness and complete automation is essential if processing and reliable interpretation of such data is to be viable. Sharp boundaries such as river beds and the top of saline aquifers must be resolved so use of smoothness constraints must be minimised. Suitable inversion algorithms must intelligently handle low signal-to-noise ratio data if conductive basement, that attenuates signal, is not to be misrepresented. A noise-level aware inversion algorithm that operates with one elastic thickness layer per electrode configuration has been coded. The noise-level aware inversion identifies if conductive basement has attenuated signal levels so that they are below noise level, and models conductive basement where appropriate. Layers in the initial models are distributed to span the effective depths of each of the geo-electric array quadrupoles. The algorithm works optimally on data collected using geo-electric arrays with an approximately exponential distribution of quadrupole effective depths. Inversion of data from arrays with linear electrodes, used to reduce contact resistance, and capacitive-line antennae is plausible. This paper demonstrates the effectiveness of the algorithm using theoretical examples and an example from a salt interception scheme on the Murray River, Australia.

Key words: geo-electric, inversion, resistivity, hydrogeology, rivers.

Introduction

Geo-electric imaging of aquifers beneath watercourses of the Murray–Darling Basin, Australia, has resulted in datasets containing millions of data points. The datasets have shown up groundwater flow paths in and out of the watercourses as well as hydrogeologically significant layering in the substrate. The datasets are useful for conjunctive groundwater and river water accounting, managed aquifer recharge and recovery scheme planning, and for identifying saline inflow into rivers. In recent years, both geo-electric and time-domain electromagnetic surveys of aquifers beneath Australian rivers have been conducted and both techniques have been refined (Barrett et al., 2003; Allen and Merrick, 2006).

Serious shortcomings and tedious quality-control procedures became evident when attempts were made to use existing inversion software to process very large geo-electric datasets. A new inversion algorithm was needed that could resolve the riverbed and the top of saline aquifers accurately, efficiently, and consistently without producing geophysical artefacts.

An introduction to geo-electric inversion

Geo-electric resistivity inversion programs attempt to automatically determine the resistivities of layers (1D inversion), prisms (2D inversion), or voxels (3D inversion) that would most accurately reproduce the observed measurements. Some 1D inversion programs additionally modify layer thicknesses in order to accurately model high-contrast boundaries present in the Earth. Various constraints, of which the smoothness constraint is most common, are applied to the inversion algorithms to prevent instability. A smoothness constraint blurs important high-contrast boundaries such as river beds and the tops of saline aquifers and therefore its use should be minimised as much as possible. Sometimes, a constraint is applied using a parameter based on the departure from *a priori* values of resistivity selected by the operator (MacInnes and Raymond, 2001). The authors have observed that constraint to a background value of resistivity produces artefacts when the *a priori* values are wrong. Therefore such a constraint should never be given much weight in towed geo-electric array surveys where robustness of inversion is of paramount importance.

Two terms must be defined to efficiently discuss geo-electric inversion. The first is the *quadrupole*, which is a pair of transmitter electrodes combined with a pair of receiver electrodes for the purpose of making one measurement of substrate apparent resistivity. Geo-electric arrays are made up of several quadrupoles, each of which has an *effective depth*; 50% of the signal received by the quadrupole is contributed by the material above the effective depth.

Effective depth centred, stretchy layer, noise-level aware inversion – an overview

The inversion scheme presented in this paper for use with towed geo-electric arrays attempts to decipher most of the information contained in the field data without adding geophysical artefacts to it (i.e. not putting false anomalous features in the interpretation). Additionally, it does this without the need for

---

*Presented at the 18th ASEG Geophysical Conference and Exhibition (AESC 2006), July 2006.

user input on a sounding-by-sounding basis, because such user input would be prohibitively costly for the volumes of data obtained typically with waterborne arrays. It is a discrete layer inversion (not a smoothed continuum of thin layers) as real stratigraphy generally has sharp boundaries, particularly at the beds of canals and rivers. The initial model is generated by centring discrete layers on all of the quadrupole effective depths of the geo-electric array used to collect the data. To more precisely model the river bed, a sharp boundary, and to reduce artefacts that may occur from forcing data to fit a smoothed resistivity model across such a boundary, one model layer boundary has been shifted to exactly match this boundary (as detected by depth sensors such as sonar or pressure devices). However, if inversion detects that for some reason the water-depth boundary has been incorrectly identified by depth sensors, perhaps because of 3D effects, then it will attempt to move the boundary to the correct depth.

Inversion proceeds to try to improve the model primarily by adjusting resistivities. However it will also try to stretch the thicknesses of layers to match any sharp boundaries that may exist. The inversion software also recognises where

conductive basement, which typically represents saline or hyper-saline aquifers, has caused signal to drop below noise level, and attempts to model such basement rather than reflect the instability of the noise.

Data may additionally be horizontally smoothed before 1D inversion, or laterally constrained during inversion (Auken et al., 2002; Santos, 2004), in order to reduce noise. Horizontal smoothing in practice produces a similar, but inferior, result to lateral constraint. It is much simpler but less elegant.

A comparison with two-dimensional inversion

Full two-dimensional smoothness-constrained inversion (e.g. Loke and Lane, 2004; MacInnes and Raymond, 2001) is not recommended for very large towed geo-electric array datasets because of serious efficiency problems as well as segment splicing and horizontal ripple problems that tend to occur in such datasets. Horizontal ripple is an observed phenomenon in which regularly spaced horizontal variation may occur spuriously in the interpretation. Some limitations of 2D inversion are evident in the example of Figure 1. The efficiency problems of 2D inversion
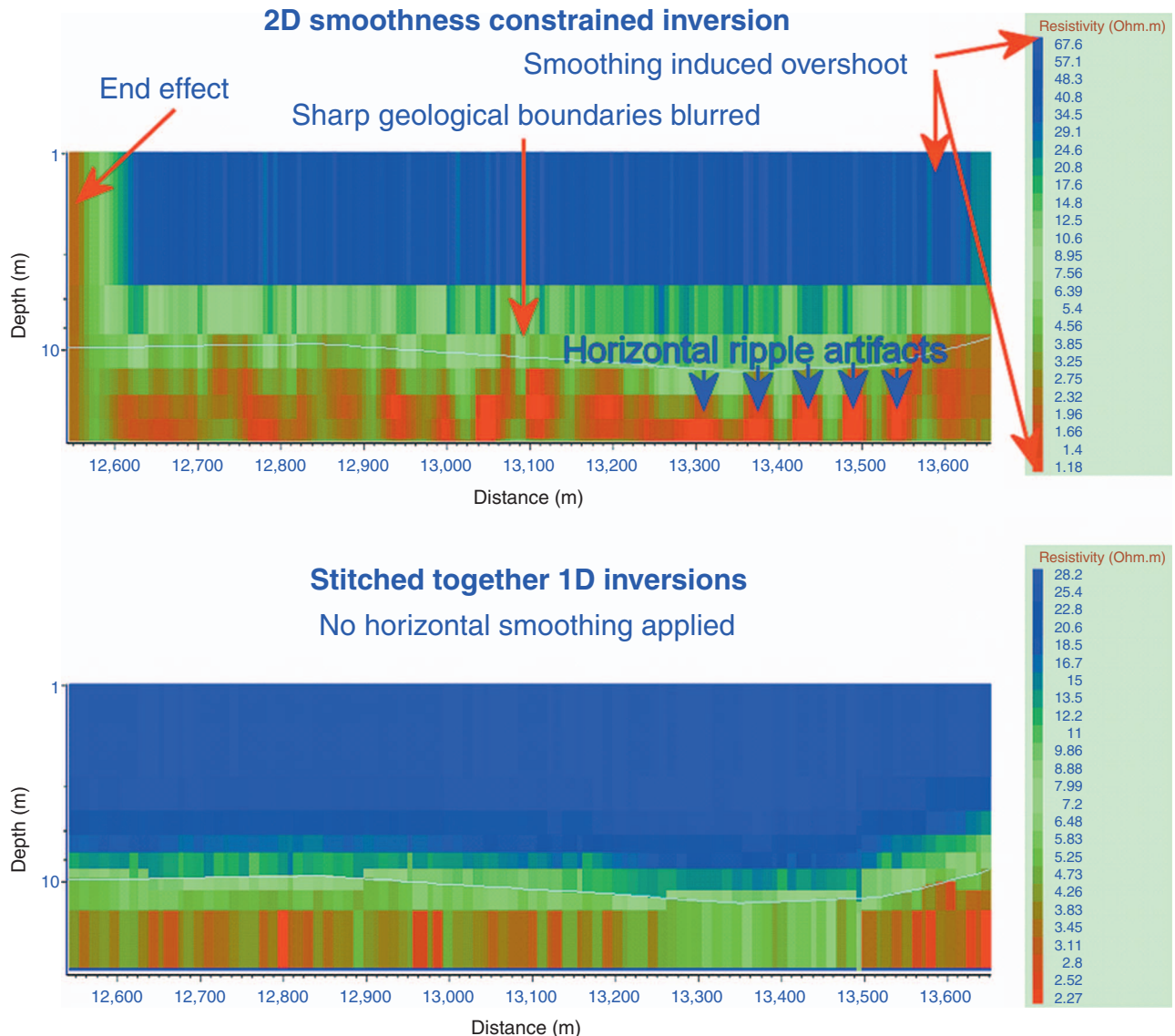
Fig. 1. A comparison of 2D and 1D inversion of one 1 km long segment of riverborne geo-electric data collected with a dipole–dipole array. An aqua line represents the approximate depth of the river bed. 1D inversion works more effectively with an array with an exponential distribution of receiver electrodes but 2D inversion of data collected with such an array is not very practical. For comparison purposes, 1D inverted data has not been horizontally smoothed as would normally be done to reduce the effect of noise.

are evident from comparison of the time taken to conduct 1D and 2D inversion. One thousand soundings (12 km of data) took 40 s to invert and image with a 3 GHz processor using the 1D algorithm presented in this paper. Two-dimensional inversion of the same amount of dipole–dipole array data was left to batch run overnight. Traditional 2D inversion of data collected using arrays with exponentially spaced receiver electrodes is much slower again, because of the small cell widths that must be used and the resultant small dataset segment size that can be inverted in one block, and the large amount of wastage of block overlap needed to remove block end effects. Two-dimensional inversion can resolve steeply dipping bodies if they are prismatic and perpendicular to the survey track but, in large towed datasets, the assumption of such prerequisites is generally not wise.

Geo-electric array and initial model selection

Effective depth centred layer inversion strategy is optimised to work with exponentially spaced towed arrays such as Allen Exponential Bipole (AXB) Arrays (Figure 2). One will not work well without the other, but the combination of the two results in nearly complete resolution of what is practically possible to resolve using a continuously towed geo-electric array travelling at reasonable speed. AXB arrays are especially designed to provide maximum resolution in towed surveys as explained in Allen and Merrick (2005). They have an approximately even distribution of quadrupole effective depths on a log depth scale because geo-electric resolution diminishes approximately logarithmically. Two linear transmitter electrodes (e.g. 0.5 m long copper tubes) are followed by receiver electrodes spaced at 2^n distance units from the end of the second transmitter electrode. The exponent n is normally incremented by 1 or 0.5. The linear electrodes are used to increase current injection. If the inversion procedure described here is used with a dipole–dipole array it will cluster initial model layers leaving little resolution near the surface. This is the best that can be done with such an inappropriate, but commonly used, array. Dipole–dipole arrays also have signal strength problems in more distant dipoles when used in towed operations. This also seriously limits vertical resolution and causes noise related inversion stability problems.

In effective depth centred layer inversion, the initial models submitted to the inversion code are composed of horizontal layers centred (on a log scale) on the quadrupole effective depths of the geo-electric array. Two layer thicknesses are then adjusted in order to place one boundary onto the bed of the watercourse as measured by sonar or pressure sensors. Resistivities of the initial model layers are set to calculated apparent resistivities. This approach permits variations in the water layer to be modelled. These variations may be genuine, or may represent geophysical artefacts. Genuine variation may be due to temperature and salinity stratification within the water column, errors in depth

detection, or to 3D undulations in the water depth beneath the geo-electric array footprint. Such artefacts in the water layer are easy to dismiss, but artefacts in the ground layer, which could be created by fixing the water layer as one discrete fixed thickness and fixed resistivity layer, can confuse interpreters. Examples of problems with the approach of fixing of the water depth and resistivity are presented by Day-Lewis et al. (2006).

Fractional signed monopole notation as a basis for inversion methodology

In order to efficiently deal with data from any geo-electric array, including arrays with linear (line source) or planar (plate source) electrodes, fractional signed monopole notation (Allen, 2006) has been adopted. A brief introduction to the notation is presented in the Appendix. New formulae, introduced in the Appendix, are integral to the inversion conducted by the authors as they allow the complications of electrode array configurations to be completely separated from the inversion code.

Forward modelling and inversion methodology

Inversion requires forward modelling of the initial and subsequent models. This is achieved using a combination of Hankel transforms and filter functions (see O'Neill and Merrick, 1984) and the signed fractional monopole approach of the Appendix.

Geo-electric inversion is appropriately solved by an iterative least absolute deviation procedure following the Marquardt algorithm for determining the approximate generalised inverse of a matrix containing derivatives of apparent resistivity with respect to each model parameter. Readers are referred to O'Neill and Merrick (1984) and Allen (2006) for a full description of the procedure.

Inversion constraints

When conducting inversion of large datasets, the inversion algorithm must be robust and automated in order to be useful. Inversion can, in a theoretical, noise-free environment, uniquely solve problems where the number of output parameters is less than or equal to the number of data points and the output parameters are linearly affected by all of the input parameters. If an AXB array is used along with effective depth centred layer initial models, then the second requirement is approximately met; however, there exist more output parameters than data points. This scenario involves modelling the same number of layers as there are data values, so the inversion needs to be stabilised with additional constraints. The problem is over-parameterised and underconstrained.

Because the inversion strategy taken involves creating an initial model with one layer per array configuration with each layer centred (on a log scale) on the effective depth of
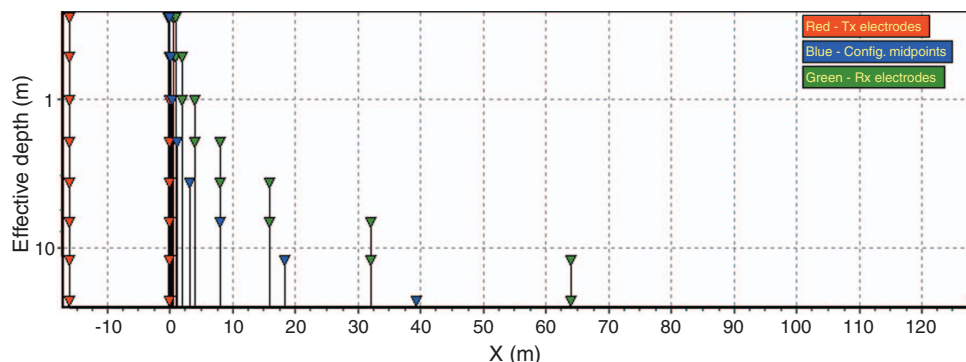
Fig. 2.   Electrode and midpoint positions (horizontal axis) of the nine quadrupoles of a particular AXB Array plotted at the respective effective depths of each quadrupole (vertical axis).

each configuration, we have nearly twice as many parameters (i.e. resistivities and thicknesses) as data. Initial attempts to stabilise inversion by fixing all the layer thicknesses resulted in geophysical artefacts in situations where high contrast boundaries were not matched exactly by model boundaries. In these situations, resistivity undershoots and overshoots occurred. Running the inversion with no fixed parameters surprisingly produced good results in some observed cases; however, in other cases, layers tended to collapse to infinitely small thickness or expand to ridiculously large thicknesses resulting in chaos. It was common for inversion to stop prematurely without changing the initial models optimally, after layers got pushed out of range or collapsed. Using fixed initial models with fewer layers proved to be inappropriate because a suitable initial model picking procedure that produced meaningful results with few layers could not be found. Addition of a minimally weighted smoothness constraint combined with a layer thickness stretch constraint, both explained below, finally solved the problems.

Stretch and smoothness constraint

A parameter representing vertical roughness of resistivity, and another representing the average degree to which layer thicknesses have been stretched from their initial model values, must be added to the sum of squares or absolute differences for the inversion to take account of stretch and smoothness. Appropriate weighting also needs to occur. The additional parameters are:

$$Roughness = \frac{wtVertSmooth \cdot \sum_{i=2}^{nLayers} \frac{2 \cdot abs(\rho_i - \rho_{i-1})}{nLayer-1}}{nLayer-1}, \quad (1)$$

and

$$Stretch = wtOrigModel \cdot \sqrt{\frac{\sum_{i=1}^{nLayers-1} \frac{sqr(t_i - toriginal_i)}{toriginal_i}}{nLayer-1}}, \quad (2)$$

where ρ_i = resistivity of layer i, t_i = thickness of layer i, $toriginal_i$ = the thickness of layer i in the initial model, $wtVertSmooth$ = weighting of the vertical smoothness constraint, and $wtOrigModel$ = weighting of the stretch constraint.

These constraints are added to the sum of squares or sum of absolute deviations as follows:

$$New\ Sum\ Of\ Squares = Sum\ Of\ Squares + Weight\ Sum \\ \times (Roughness + Stretch)$$

$$New\ Sum\ Of\ Abs\ Dev = Sum\ Of\ Abs\ Dev + Weight\ Sum \\ \times (Roughness + Stretch).$$

Note that the function sqr() may be interchanged with the function abs() in both equations, but sqr() is always better in equation (2) because it is not desirable for the layers to stretch very far and also not desirable to unduly restrict small amounts of stretch. It is better for the layer above or below to start changing thickness in order to better match the data than for a layer to be stretched so much that it overlaps the original boundaries of adjacent layers in the initial model.

In order to resolve the large resistivity contrasts at boundaries common in towed waterborne data, it is important to keep *wtVertSmooth* as small as possible and compensating by increasing *wtOrigModel*. The stretch constraint alone cannot however stabilise the overparameterised models that are being generated, as it has no ability to constrain layer resistivities. It has been found, by trial and error, that, with a typical AXB array, a combination of a value of 0.01 for *wtOrigModel* and a value for *wtVertSmooth* of 0.1 (when

conducting L1 norm inversion) or 0.05 (for L2 norm inversion) is optimal.

Dealing with noise

Sub-noise data aware inversion

Highly conductive units such as sulphide ore bodies, aquifers containing hyper-saline groundwater, and thick saline clays attenuate much of the signal available to geo-electric arrays. The lack of signal does not imply that the data is useless but rather that the anomalies are very conductive. This implication should be taken into consideration in inversion otherwise inversions over conductive features will be erratic and misleading. A similar, but generally non-problematic, situation exists when transient electromagnetic signals decay rapidly when sensing extremely resistive half spaces.

The sub-noise data aware inversion technique attempts to recognise data that is below noise level and proceeds by constraining inversion to models that would create such sub-noise data. Such an approach will honour data that is above noise level and invert it correctly, while also modelling conductive anomalies to the minimum conductivity that would keep data below noise level. The problem is more pronounced in cases where density of sampling with depth is poor, such as with many pulled array surveys in which electrodes have been spread widely in order to increase signal levels to permit faster sampling. Existing algorithms inverting high vertical density geo-electric datasets (i.e. datasets with lots of points with effective depths within each decade of depth) are likely to model conductive features using data from quadrupoles with effective depths just above the features. If such algorithms are inverting low vertical density datasets then they will either barely detect such conductive features or completely miss them.

A full explanation of the algorithm follows. Least norm inversion (such as least-squares inversion) tries to minimise a sum of errors between model and field data. It is common practice to weight such errors so that field data with low signal to noise levels have little influence on the sum of errors. In sub-noise data aware inversion, field and model data below noise level are prevented from inappropriately influencing the sum of errors. To begin, a noise level is identified, either by an operator who has analysed a sample dataset or by an instrument that, theoretically, can automatically detect noise levels. Then the algorithm laid out in Figure 3 is executed for each data point i within each sounding during each iteration of the inversion process.
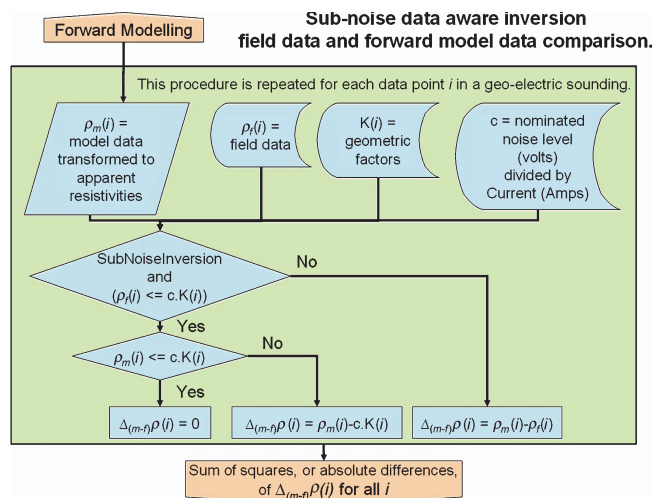

Fig. 3. Flow chart for sub-noise data aware inversion field data and forward model data comparison.

The technique differs from standard inversion in that, if both model and field data are below the nominated noise level then the difference between them is recorded as zero so that the model is considered to be a valid model by the inversion criterion. If only the model data point is above noise level then the inversion criterion only penalises according to difference between the model data and the noise level.

Coded in Pascal, the algorithm described above appears as follows:

```
If SubNoiseInversion and (RField[i] <=
  NoiseDivCurrent*GeomFact[i]) then
    If RModel[i] <= NoiseDivCurrent*
      GeomFact[i] then
        ModelMinusField[i] := 0
    else
        ModelMinusField[i] := RModel[i]-
          NoiseDivCurrent*GeomFact[i]
  else ModelMinusField[i] := RModel[i]-
    RField[i];
```

where `RField(i)` represents a field apparent resistivity and `RModel(i)` represents a forward modelled solution for a layered model, and is calculated in each iteration of the inversion algorithm. For each sounding, the noise level is divided by current injected to give `NoiseDivCurrent`.

That is all that is needed to resolve conductive basement using geo-electric data that falls below noise level. It is not possible to tell how conductive the basement is, however, just that it is conductive enough to force the field data to less than the noise level. Some minor erratic representation of the basement conductivity will still be evident due to noise spikes that exceed the nominated noise level. Sub-noise data aware inversion does not try to provide a solution for where geo-electric arrays cannot 'see' any more than conventional inversion but rather simply stably inverts data, ignored by conventional inversion, that definitely is indicating the presence of conductive basement. If there is no conductive basement but some data still falls below noise level, then sub-noise data aware inversion simply will not try to vary the part of the initial model that is beyond detection.

Weighting of data depending on signal-to-noise ratio

Data point weights may be determined from RMS or sum-of-square calculations within the inversion code. Such weighting procedures increase the stability of the inversion routine but must be conducted with moderation. Weighting is not an alternative to sub-noise data aware inversion because excessive weighting can generate the same type of artefacts that sub-noise data aware inversion attempts to remove. A moderate amount of data weighting dependent on signal-to-noise ratios can appropriately be used in conjunction with noise-aware inversion.

Weighting may be applied as follows:

1. The following parameters may be input by the user: *WeightLimit* (the maximum voltage at which weight is diminished), *Noise* (the voltage at or below which minimum weight is applied; this is obtained by observing sample data), and *WeightAtNoise* (the weight at or below noise voltage).
2. Above *WeightLimit*, a weight of 1 may be applied; and
3. Between *WeightLimit* and *Noise*, a weight may be linearly applied using

$$Weight = WeightAtNoise + (1 - WeightAtNoise)$$
$$\times \frac{V[i] - Noise}{WeightLimit - Noise}. \qquad (3)$$

In sub-noise data aware inversion weights of data below noise level are insignificant. Weights of data just above noise level will, however, be significant and, if they are appropriate, will smooth and enhance inversion more than unweighted sub-noise data aware inversion.

Inversion methodology verification using stitched three-layer theoretical models

Effective depth centred stretchy layer inversion

Stitched sets of theoretical three-layer models were created for the purpose of testing inversion algorithms. In order to reflect the types of models encountered under rivers, layer 1 was fixed at 100 Ω m, layer 2 was varied from 1000 to 0.1 Ω m in five steps, and layer 3 was fixed at 1 Ω m. For each of these five sets of layer resistivities, eleven variations of thickness of layer 1, from 0.5 to 5 m, were generated. The thickness of layer 2 was set as 2 m and layer 3 thickness was infinite. All were plotted, stitched together, in a coloured vertical section as shown in Figure 4a. Note that the horizontal axis of the section is 'Sounding Number' rather than distance and that each model is one-dimensional. For all of these models, forward modelled datasets were created for a 144 m long AXB floating array.
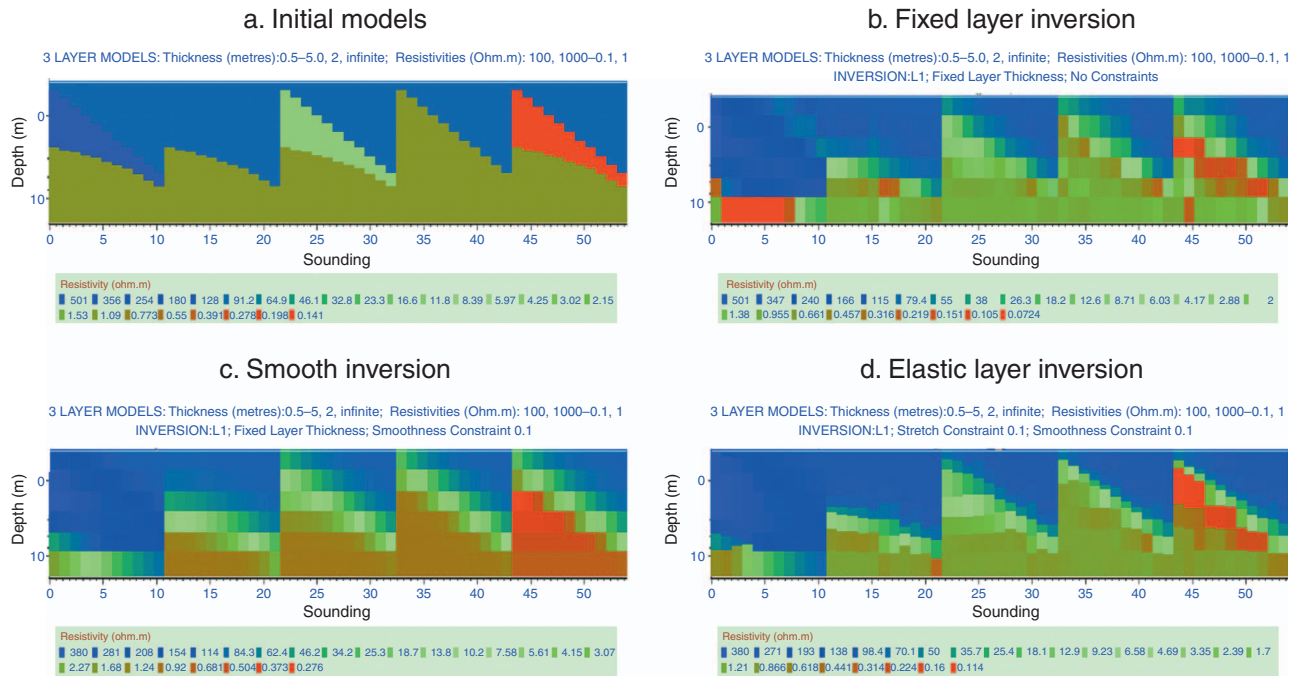
It is possible to simply plot apparent resistivities versus effective depths in order to replicate the models in a blurred manner; however, in cases where strong resistivity contrasts exist, apparent resistivity images are not optimal. Sharp features are blurred and thicknesses of anomalously conductive or resistive layers appear incorrectly. In waterborne surveys, detail at the river bed (typically a high-contrast boundary) is important and therefore inversion is recommended. Simple fixed-layer inversion in which one layer is created for each effective depth in an array is shown in Figure 4b. This type of inversion works well over smoothly varying layered models but creates excessively high or low resistivity layers (geophysical artefacts) over high-contrast boundaries when the high-contrast boundary does not match a fixed layer boundary exactly. In Figure 4b an example of such an artefact exists and is clearly evident on the left side of the image as a high-conductivity basement.

Fixed layer inversion code such as used to generate Figure 4b may operate well in many, but not all, situations. In order to avoid this instability, most inversion specialists resort to creation of numerous thin layers which they constrain using a vertical roughness parameter. An example of smoothness-constrained fixed layer thickness inversion is presented in Figure 4c. The result differs little from an image of apparent resistivity plotted against effective depths.

Rather than increasing the number of layers, the inversion code may be constructed to stretch thicknesses of modelled layers in order to fit data better. Layer thicknesses were floated and a stretch constraint, along with a little smoothness constraint, were added (in proportions recommended earlier in this paper) giving the result shown in Figure 4d. The smoothness constraint was applied using L1 (least absolute deviation) inversion rather than L2 (least squared deviation) inversion because the L1 norm damps roughness outliers (high conductivity contrast boundaries) less.

Sub-noise data aware inversion

Investigation of saline inflow into rivers involves another inversion challenge – extremely conductive basement which absorbs signal resulting in data that must be either clipped at a noise level or processed using sub-noise data aware inversion.

a. Initial models

3 LAYER MODELS: Thickness (metres):0.5–5.0, 2, infinite; Resistivities (Ohm.m): 100, 1000–0.1, 1

Resistivity (ohm.m)

b. Fixed layer inversion

3 LAYER MODELS: Thickness (metres):0.5–5.0, 2, infinite; Resistivities (Ohm.m): 100, 1000–0.1, 1
INVERSION:L1; Fixed Layer Thickness; No Constraints

Resistivity (ohm.m)

c. Smooth inversion

3 LAYER MODELS: Thickness (metres):0.5–5, 2, infinite; Resistivities (Ohm.m): 100, 1000–0.1, 1
INVERSION:L1; Fixed Layer Thickness; Smoothness Constraint 0.1

Resistivity (ohm.m)

d. Elastic layer inversion

3 LAYER MODELS: Thickness (metres):0.5–5, 2, infinite; Resistivities (Ohm.m): 100, 1000–0.1, 1
INVERSION:L1; Stretch Constraint 0.1; Smoothness Constraint 0.1

Resistivity (ohm.m)

Fig. 4. A comparison, using data computed from a stitched three-layer model, between unconstrained fixed layer thickness inversion, smoothness constrained inversion, and elastic layer thickness constrained inversion. Note that the horizontal scale is sounding number – these are not 2D sections. (a) Stitched together three-layer models, from which data were computed for inversion in panels (b), (c), and (d). (b) Fixed layer thickness inversion with one layer per effective depth of a 144 m AXB array. Note the artefact of conductive basement near the left side. (c) Smoothness constrained inversion with layers of fixed thickness centred on the effective depths of the 144 m AXB array. (d) Stretch and smoothness constrained inversion of layers centred on the effective depths of the 144 m AXB array. Seemingly random variations in the section are actually a result of instability resulting from the phenomenon of equivalence.
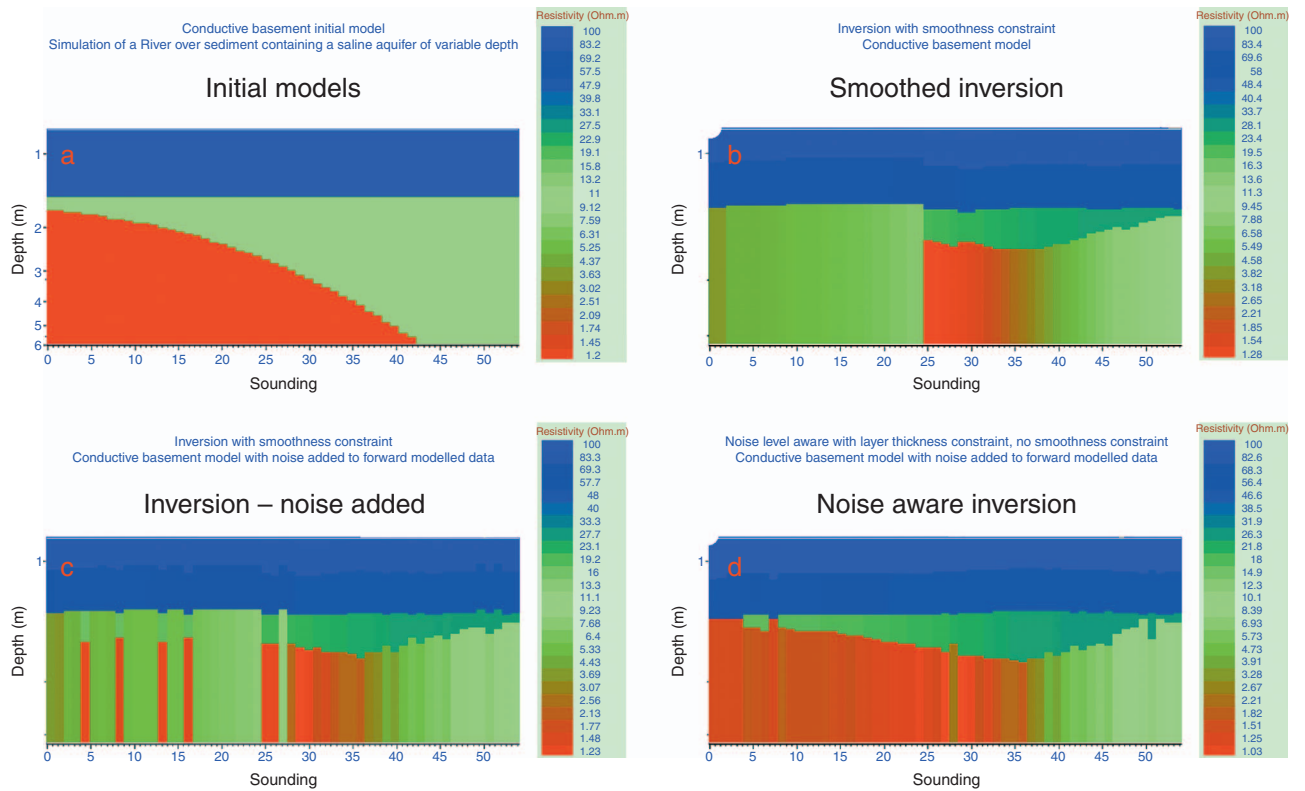
Fig. 5. A comparison, using data computed from a stitched three-layer model, between inversion that is aware of, and unaware of, noise levels. Note that the horizontal scale is sounding number – these are not 2D sections. (a) Stitched together three-layer conductive basement models simulating a river over sediment containing a saline aquifer of variable depth, from which data were computed for inversion in panels (b), (c), and (d). (b) Inversion of data, clipped at noise level, collected over the models of Figure 5a. Note the disconcerting loss of detection of conductive basement on the left. (c) Inversion of data clipped at noise level as for Figure 5a but with random noise added to the forward modelled data. Note again that the conductive basement is only sporadically detected on the left. (d) Sub-noise data aware inversion with stretch constraint and minimal smoothness constraint. The result is very similar to the initial models.
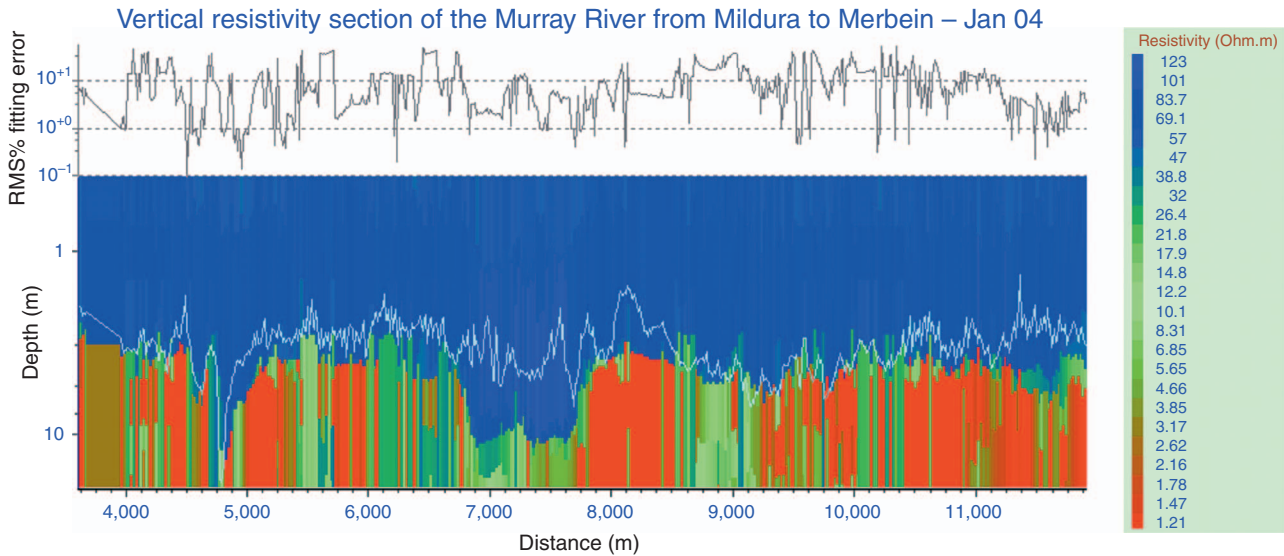
Fig. 6. An example of inverted geo-electric array data collected at a part of the Murray River where hypersaline groundwater is just below the river bed. The hypersaline groundwater has consumed signal and resulted in artefacts in the data where inversion has been destabilised by low signal-to-noise ratios and data clipping. This image extends from Mildura downstream.
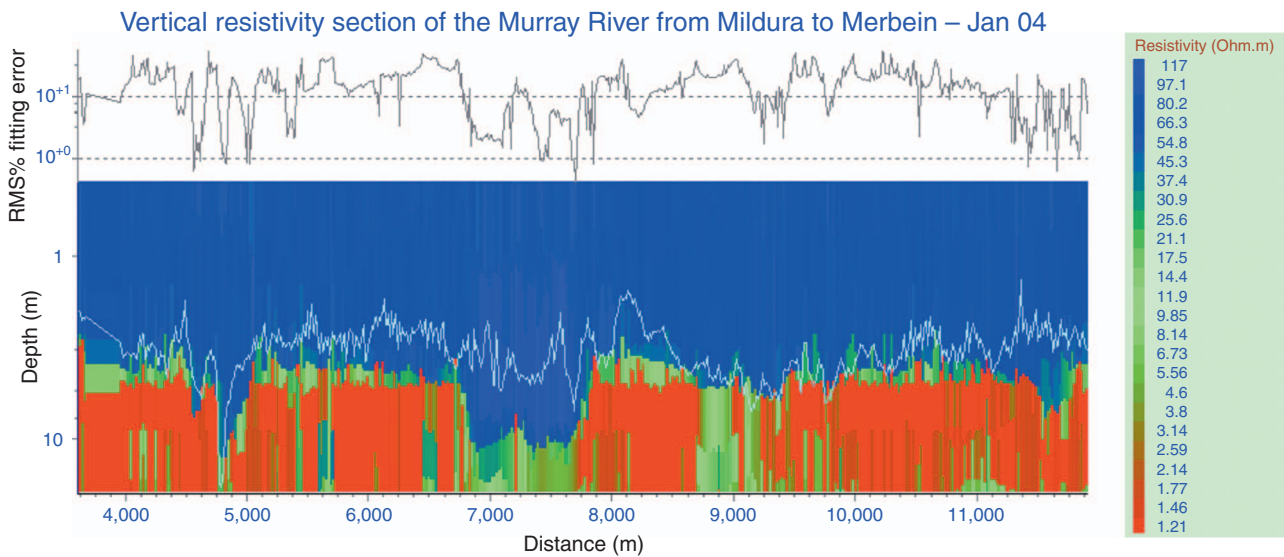
Fig. 7. The same data as Figure 6 re-inverted using noise-level aware inversion. Most of the artefacts are now eliminated.

Clipping of different soundings at different data-points creates instability in standard inversion software. Sub-noise data aware inversion was invented to deal with this instability. The stitched three-layered models shown in Figure 5a were produced to demonstrate the performance of sub-noise data aware inversion. Layer resistivities were set at 100, 10, and 1 Ω m. Layer 1 thickness was set at 1.4 m while layer 2 thickness was varied from 0.2 to 10 m in small steps.

If the forward-modelled datasets produced from these models were clipped at a noise level and then plotted as apparent resistivity versus effective depth it would erroneously appear as if the conductive basement disappears on the left side of the image.

Once the data, clipped at noise level, have been modelled conventionally, the serious geophysical artefact observed in Figure 5b occurs. Conductive basement has not been resolved in those soundings where conductivity has increased with respect to depth so abruptly that it has left no points above noise level that are affected by the conductive basement.

Although the theoretical data in Figure 5b has been clipped at a nominated noise level, being theoretical data, it has no noise. The same inversion procedure that created Figure 5b was repeated on a dataset created by adding randomly generated noise to the forward modelled data before clipping it at the noise level. Standard inversion of such data resulted in an image with geophysical artefacts as shown in Figure 5c.

Sub-noise data aware inversion removes such artefacts as shown in Figure 5d, limiting conductivities to values that would generate data below the noise level.

In Figures 5b, 5c, and 5d, the basement interface is seen to climb to the right on the right side of the figures, while the basement conductivity approaches that of layer 2 of the initial models. This has happened where the conductive basement is well below the effective depth of the last configuration in the array used. It is a result of the transition between where basement is represented by layer 3, to where it is represented by layer 2, of the initial models.
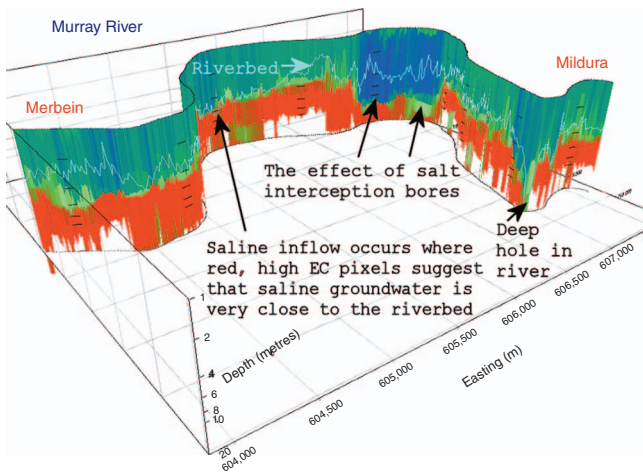
Fig. 8. Three-dimensional presentation of the model in Figure 7. This presentation method is necessary as a plain vertical section is very hard for interpreters to compare with the locations of known geological and cultural features.

Inversion methodology verification using a Murray River saline inflow site example

The Murray River near Mildura, South-East Australia, is underlain by upward-flowing saline and hypersaline groundwater. Salt interception bores extract some of this groundwater, preventing it from flowing up into the river. Geo-electric imaging has been used to determine where the pumping is effective, and where it is not. It also has been used to resolve geological features that may be affecting groundwater flow.

The hypersaline groundwater absorbs signal resulting in noisy data. Figure 6 shows the result of modelling such data without using sub-noise data aware inversion. By comparing Figure 6 with Figure 7, modelled using sub-noise data aware inversion, one can see that numerous anomalies in Figure 6 are artefacts. It is clear that data from such areas, processed without noise-level aware inversion, is confusing at best. In Figure 7, proximity of the saline groundwater to the riverbed, detected using sonar and represented by an aqua line, is clear, as is freshwater drawdown around some of the salt interception bores. Quality of the inversion is evident from its ability to honour the almost constant conductivity in river water and the high conductivity contrast across the riverbed that exists at places where salt interception bores have little effect. The riverbed was detected independently using sonar and left to float in the inversion. Figure 8 presents the same data in three dimensions so that geological and cultural features of interest can be located on, and compared to, the imagery.

Conclusions

Effective depth centred, stretchy horizontal layer, sub-noise data aware, L1 norm inversion with minimal smoothness constraint and some weighting of data according to signal to noise ratio is almost ideal for towed geo-electric array data processing. Some additional improvement can be made by horizontally smoothing or laterally constraining the data. Inversion of waterborne geo-electric data can be enhanced by moving the initial model layer boundary that is closest to the water depth, obtained independently, onto the water depth. Combination of such inversion with use of an array with a good distribution of effective depths is recommended for towed geo-electric surveying.

References

Allen, D. A., 2006, *Electrical Conductivity Imaging of aquifers connected to watercourses, A thesis focussed in the Murray Darling Basin, Australia*: PhD Thesis, University of Technology Sydney.

Allen, D. A., and Merrick, N. P., 2005, Towed geo-electric arrays for analysis of surface water groundwater interaction: *Proceedings of the Symposium on Applications of Geophysics to Engineering and Environmental Problems conference*.

Allen, D. A., and Merrick, N. P., 2006, Aquifer and watercourse interaction in the Murray–Darling Basin elucidated using electrical conductivity imaging: *18th Geophysical Conference and Exhibition, Australian Society of Exploration Geophysicists*, *Extended Abstracts*.

Auken, E., Foged, N., and Sorensen, K. I., 2002, Model recognition by 1-D laterally constrained inversion of resistivity data: *9th Meeting, Environmental and Engineering Geophysical Society-European Section, Proceedings*, 241–244.

Barrett, B., Hatch, M., Heinson, G., and Telfer, A., 2003, Salinity monitoring of the Murray River using a towed TEM array: *16th Geophysical Conference and Exhibition, Australian Society of Exploration Geophysicists, Extended Abstracts*.

Day-Lewis, F. D., White, E. A., Johnson, C. D., Belaval, M., and Lane, J. W., Jr, 2006, Continuous resistivity profiling to delineate submarine groundwater discharge – examples and limitations: *The Leading Edge* **25**, 724–728. doi:10.1190/1.2210056

Loke, M. H., and Lane, J. W., 2004, Inversion of data from electrical imaging surveys in water-covered areas: *Exploration Geophysics* **35**, 266–271.

MacInnes, S., and Raymond, M., 2001, *TS2DIP – Smooth-Model Resistivity and IP Inversion with topography version 4.00*, Zonge Engineering and Research Organization, Inc.

Merrick, N. P., 1997, A new resolution index for resistivity electrode arrays: *Exploration Geophysics* **28**, 106–109.

O'Neill, D. J., and Merrick, N. P., 1984, A Digital Linear Filter for Resistivity Sounding with a Generalized Electrode Array: *Geophysical Prospecting* **32**, 105–123. doi:10.1111/j.1365-2478.1984.tb00720.x

Roy, A., and Apparao, A., 1971, Depth of investigation in direct current methods: *Geophysics* **36**, 943–959. doi:10.1190/1.1440226

Santos, A. M., 2004, 1-D laterally constrained inversion of EM34 profiling data: *Journal of Applied Geophysics* **56**, 123–134. doi:10.1016/j.jappgeo.2004.04.005

Appendix: An introduction to fractional signed monopole notation

Fractional signed monopole notation, introduced by Allen (2006), is suitable for generalizing geo-electric array formulae. It divides the signal coming from quadrupoles into signed monopole portions and combines them using the principle of superposition, which is valid in geo-electric theory (O'Neill and Merrick, 1984). Signed proportions are, for point electrode arrays, simply the product of the signs of the transmitter and receiver electrodes relevant to each monopole. As long as one of each type (i.e. transmitter or receiver) is allocated as positive, and the other as negative, the equations work. For arrays with linear electrodes, the signed proportions are the product of a sign (polarity), as explained, but also a fraction dependent on how the linear electrodes have been segmented. By strategically segmenting the electrodes, for each quadrupole, it is possible to process data from arrays containing moderate length linear electrodes, or even plate electrodes, in little more than the time needed to process data from point electrode arrays (Allen, 2006). Potential for use of the same technique with capacitive line and plate antennae is obvious.

Apparent resistivities are determined using the following equations. First we must calculate the geometric factor for the array, which is determined as follows:

$$K = \text{abs}\left(\frac{2\,\pi}{\sum_{i=1}^{n}\frac{p_i}{r_i}}\right) \tag{A1}$$

where K = geometric factor, n = number of monopoles (i.e. the number of receiver electrode–transmitter electrode combinations), $\sum_{i=1}^{n}$ = summation over the set of inter-electrode distances and proportions (simplifies to $i = 1$ to 4 for standard four-point electrode arrays), r_i = i-th inter-electrode distance, and p_i = signed proportion for inter-electrode distance i.

The apparent resistivity of a surface array configuration is then given by

$$\rho_a = \frac{K\,\Delta V}{I} \tag{A2}$$

where ΔV = voltage difference measured between potential electrodes, and I = current flowing through current electrodes.

The logic and simplicity of the new notation may be easier to understand through an example. Using conventional notation, the apparent resistivity for an α-Wenner array with an inter-electrode spacing of a would be defined as

$$\rho_a = \frac{\Delta V}{I}\,\text{abs}\left(\frac{2\,\pi}{\frac{1}{r_{11}} + \frac{1}{r_{22}} + \frac{1}{r_{12}} + \frac{1}{r_{21}}}\right)$$

where $r_{11} = a$, $r_{22} = a$, $r_{12} = 2a$, and $r_{21} = 2a$.

Using the new notation, apparent resistivity would be defined as:

$$\rho_a = \frac{\Delta V}{I}\,\text{abs}\left(\frac{2\,\pi}{\sum_{i=1}^{n}\frac{p_i}{r_i}}\right)$$

where $n = 4$, $r_1 = a$, $r_2 = a$, $r_3 = 2a$, and $r_4 = 2a$, $p_1 = 1$, $p_2 = 1$, $p_3 = -1$, and $p_4 = -1$.

When dealing only with α-Wenner array data, the new notation would not be of significant advantage, but this example is given to help readers understand how the advantage of the new notation can become very significant when generalisation is necessary and the complications of elaborate array configurations must be kept independent of inversion code.

Inversion methodology explained by this paper requires calculation of effective depths which are obtained by discretely integrating NDIC(z), the normalised depth of investigation characteristic, in logarithmic increments, until the integral just exceeds 0.5 (Merrick, 1997).

$$0.5 = \int_{z=0}^{z\,\text{effective}} \text{NDIC}(z)\,\mathrm{d}z \tag{A3}$$

The formula for NDIC(z) for any array lying on the surface of a half space is

$$\text{NDIC}(z)_{\text{surface}} = 4z\,\frac{\sum_{i=1}^{n}\frac{p_i}{(r_i^2+4z^2)^{3/2}}}{\sum_{i=1}^{n}\frac{p_i}{r_i}}\,\mathrm{d}z \tag{A4}$$

where z = depth in metres (a range of 10^{-2} to 10^3 can be sampled as this effectively covers the depth of investigation of most arrays), $\mathrm{d}z$ = a small increment in z (increments of 10^n have been used where $n = 0.001$).

Derivations of these formulae are completed in Allen (2006) by generalising the derivations of the same formulae, derived for specific cases, by Roy and Apparao (1971).

水文地質学研究に利用される牽引式アレイ電気探査大規模データのロバスト1次元逆解析

D. アレン[1]・N. メリック[2]

要　旨：　陸上および水上の牽引式アレイ電気探査法の出現は，空中電磁探査に匹敵する大規模データセットをもたらし，その解析には1次元逆解析の適用が最も適している。そのような大規模データの処理や信頼できる解釈を実現可能にするためには，ロバスト（頑健）で完全自動の逆解析手法が必要不可欠である。河床や塩水性帯水層の地下水面のような明瞭な境界を捉えなければならない場合，平滑化の拘束条件の使用は最小限に抑えられなければならない。信号を減衰させるような導電性の基盤を正確に把握する場合，低SN比データを上手く処理する逆解析アルゴリズムが適切である。我々は，個々の電極配置に対して一つの融通性のある層厚を持つ層を仮定する，ノイズレベルは既知とした逆解析アルゴリズムをプログラム開発した。この逆解析法は，導電性の基盤が信号レベルを減衰させ，それがノイズレベル以下になったかどうかを特定し，導電性基盤を適切な場所に作成する。初期モデルにおける層は，それぞれのアレイ4極子に対応する影響深度に達するように配置される。アルゴリズムは，指数関数的に影響深度が分布するような電気探査アレイで取得したデータに対して最適に動作する。接地抵抗を低減するために利用される線状電極や，キャパシタ線アンテナを用いたアレイで取得したデータの逆解析には，適しているようである。本論文では，理論的な実験例とオーストラリア マレー川の塩害阻止事業の例に対するアルゴリズムの有効性を示す。

キーワード：電気探査，逆解析，比抵抗，水文地質学，河川

수리지질학 연구에 이용되는 대규모 끄는 방식 전기비저항 배열 자료의 1차원 강력한 역산

David Allen[1], Noel Merrick[2]

요　약：　물위나 육지에서 *끄*는 방식의 전기비저항 배열법의 등장은 그 자료량의 규모를 항공전자탐사의 규모에 가깝게 만들었으며, 이렇게 얻어진 자료들의 대부분은 해석을 위한 1차원 역산이 시도되었다. 이 자료들의 믿을만한 해석과 자료처리를 실행 가능화시키기 위해서는 강력하고 완벽한 자동화 공정은 필수 불가결한 요소이다. 하상이나 염수 대수층의 상부와 같은 뾰족한 경계를 찾아내야 하므로 평활화제한법의 이용은 최소화 시켜야 한다. 적절한 역산 방식이라면 신호를 감쇠시키는 전도성 기반암의 경우에는 해석의 오류를 피하기 위해 낮은 신호대 잡음비를 현명하게 다룰 수 있어야 한다. 이를 위해 각각의 전극 배열법에 대해 하나의 탄력적 두께를 갖는 층을 운용하는 잡음 인지 역산 방법이 코딩되었다.　잡음 인지 역산법은 만약 전도성 기반암이 신호를 감쇠시켜 잡음 수준보다 작게 만들면 이를 감지하여 적당한 위치에 전도성 기반암을 갖는 모형을 구성해 준다. 초기모형의 층들은 4극으로 구성된 각 전기 배열법의 유효깊이가 미치는 범위 내에서 제 위치를 찾아가게 된다. 이 알고리듬은 4극의 유효깊이가 대략 지수함수적인 배열을 이루어 자료가 얻어졌을 때 가장 최상의 결과를 나타낸다. 접지저항을 줄이기 위한 선전극이나 용량선 안테나 (capacitive-antenna)에 의한 자료의 역산도 가능하다. 이 논문은 이론자료와 오스트레일리아의 Murray 강의 염분차단 계획의 예를 들어 개발된 알고리듬의 유용성을 보여주었다.

주요어：지구 전류, 전기비저항, 수리지질학, 강

1 地下水イメージング（株）
2 シドニー工科大学，地下水管理研究センター

1 지하수 영상화 ㈜
2 지하수관리국립센터, 시드니 기술대학